



## Cyclic plasticity investigations including ratchetting and hardening under nonproportional loadings - Experiments and modeling

Portier L.<sup>(1)</sup>, Colloch S.<sup>(2)</sup>, Geyer P.<sup>(1)</sup>, Marquis D.<sup>(2)</sup>

(1) EDF, France

(2) ENS Cachan / LMT, France

**ABSTRACT:** This paper is concerned with the ratchetting behaviour of 316 Stainless Steel under nonproportional tension-torsion loadings at room temperature. Two tension-torsion tests are carried out with bowtie type loadings combining simultaneous cycling of axial stress and shear strain. Next, we compare the performance of five phenomenological cyclic plasticity models in predicting the experimental results.

### INTRODUCTION

In many engineering applications, structures in 316 Austenitic Stainless Steel can be submitted to cyclic loads in the inelastic domain which can create a cumulative inelastic deformation or ratchetting of structure under the combination of a primary constant load and a secondary cyclic one. In such a case, it can lead to degradation and failure due to accumulation of deformation. Therefore this problem has received considerable attention over the last twenty years. It has led to the development of a significant number of models of cyclic plasticity to predict the ratchetting of structures. In addition, several ratchetting tests on homogeneous specimen have been developed to elaborate these models; namely, tension-torsion tests and axial-internal pressure tests in a presence of a mean stress. Up to now, these models exhibit quite good agreement with simple ratchetting tests but usually fail to describe the ratchetting observed in structures where the loadings are more complex. Therefore the main goal of our work is to discriminate these models on complex tension-torsion loadings on homogeneous specimen. In the first part of our paper, we present two complex tension-torsion tests of bowtie type on 316 Stainless Steel tubes at room temperature. The second part of the paper is concerned with the modeling of ratchetting: we evaluate the performance of five different phenomenological plasticity models in predicting the experimental results.

### EXPERIMENTAL PROGRAM

#### *Experimental equipment*

Experiments are carried out on thin walled 316 Stainless Steel tubular specimen at room temperature. The geometry is described in figure 1. The material is type 316 Stainless Steel. The chemical composition is given in table 1. The machine used is a MTS axial-torsion servohydraulic testing machine. The acquisition operations and command signal generation are made by a Macintosh Quadra 950 equipped with a N.B.MIO.16 card and a N.B.AO.6 card and Labview software. Axial and shear strains are measured by strain gages of rosette type (VISHAY MMEP-08-125RA-120). Axial and shear stresses are obtained by corresponding load cells.

C	S	P	Si	Mn	Ni	Cr	Mo	Cu	Fe
0.016	0.020	0.025	0.65	1.78	11.4	17.00	2.02	0.25	balance

Table 1 : Chemical composition of the 316L Austenitic Stainless Steel (% in volume)

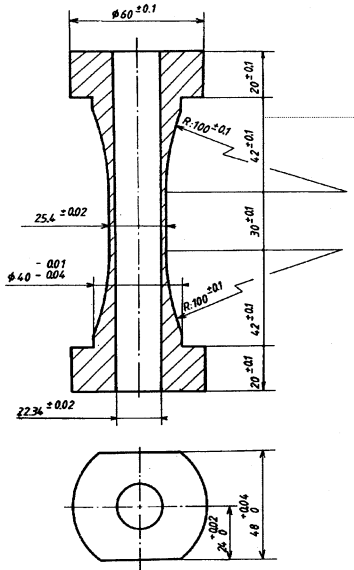


Figure 1 : Geometry of the specimen

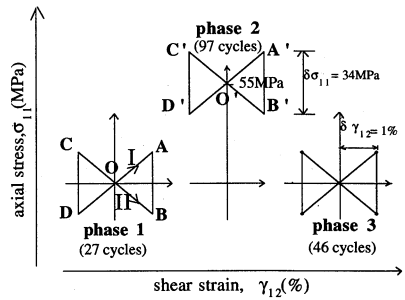


Fig. 2: Imposed axial stress-shear strain path. path I - path II

### Description of loading paths

The two studied paths are bowtie type. Each of the two paths consists of three sequences at different mean stress and a constant shear strain amplitude of 1%. The difference between path I and path II is depicted in figure 2. Namely, path I begins with an increasing of the axial stress (OABCD), conversely, path II begins with a decreasing of the axial stress (OBADC). In the first phase, a zero mean stress is imposed for 27 cycles up to the steady state (phase 1). Next, the shape of the path is kept but a mean stress of 55MPa is imposed for 97 cycles (phase 2). Endly, the shape of the path remains unchanged and the mean stress is suppressed at zero mean stress for 46 cycles (phase 3).

### Experimental results

Figure 4 shows a plot of the maximal axial strain over each cycle versus the number of cycles for both path I and path II. Figure 4 and 5 show the axial-shear strain response for path I and path II during phase 1 and 2 and figure 6 and 7 show the axial-shear stress response for path I and path II during phase 1 and 2.

Though a zero mean stress is imposed in phase 1, path I produces a small ratchetting of the axial strain and path II leads to a small negative ratchetting of the axial strain (see figure 3). During this phase the specimen is cyclically stabilized in 20 cycles. Next, due to their non zero mean stress during phase 2, both path I and path II produce ratchetting of the axial strain (see figure 5 and 6). This ratchetting is somewhat faster for path I (see figure 3). During this phase we observe no hardening of the shear stress (see figure 6 and 7). Finally, we observed in phase 3, for both path I and II a partial recovery of the axial strain at the same rate (see figure 3).

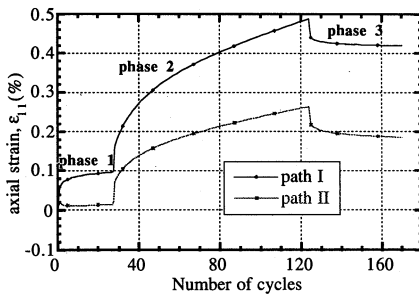


Fig. 3 : Maximal axial strain over a cycle versus the number of cycles  
path I- path II.

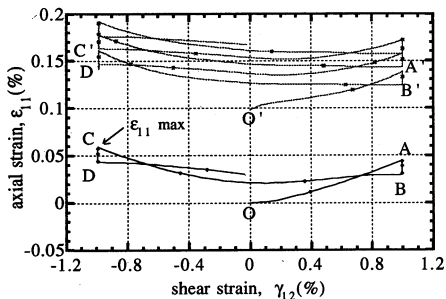


Fig. 4: axial - shear strain response for path I.  
- OABCD: first cycle - phase 1  
- O'A'B'C'D': beginning of phase 2

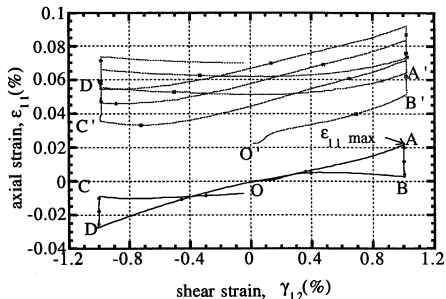


Fig. 5: axial - shear strain response for path II.  
- OABCD: first cycle - phase 1  
- O'A'B'C'D': beginning of phase 2

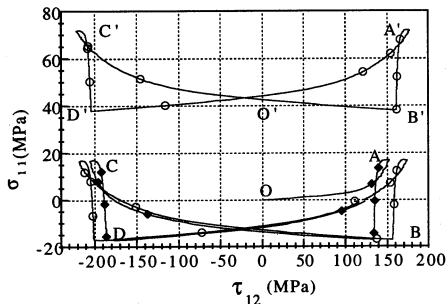


Fig. 6: axial - shear stress response for path I.  
- OABCD: first and last cycle - phase 1  
- O'A'B'C'D': last cycle - phase 2

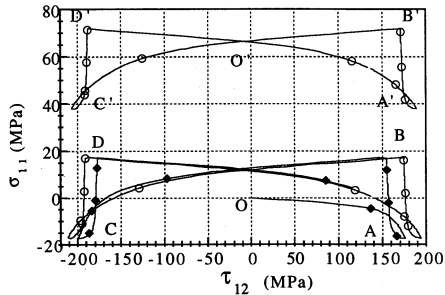


Fig. 7: axial - shear stress response for path II.  
- OBADC: first and last cycle - phase 1  
- O'B'A'D'C': last cycle - phase 2

CONSTITUTIVE MODELING

Different constitutive equations are used to predict these tests. Namely, we use five phenomenological models. The cyclic constitutive equations are studied in term of hierarchy of various models. The basic model for the simulations is a cyclic plasticity model with one isotropic hardening rule and two non linear kinematic hardening rules (Armstrong Frederick type) (Chaboche [1]). Then, we studied two modifications in kinematic hardening rules superimposed to this basic model to improve the decription of ratchetting (the model proposed by Burlet-Cailletaud [2] and used by Geyer [3], the model proposed by Ohno [4]) and two modifications in isotropic rule superimposed to the basic NLK model to improve the description of the nonproportionality effect (the model proposed by Benallal-Marquis [5] and modified by Calloch [6], the model proposed by Tanaka [7]). The corresponding constitutive equations are presented in the following:

-The model proposed by Chaboche [1], elastoplastic formulation (named NLK model):

- Strain partition :  $\underline{\underline{\epsilon}} = \underline{\underline{\epsilon}}^e + \underline{\underline{\epsilon}}^p$  (1)
- Elastic domain :  $f(\underline{\underline{\sigma}}, R, \underline{\underline{X}}) = J_2(\underline{\underline{\sigma}} - \underline{\underline{X}}) - R - k$  (2)
- $J_2(\underline{\underline{\sigma}} - \underline{\underline{X}}) = \sqrt{\frac{3}{2} (\underline{\underline{S}} - \underline{\underline{X}}) : (\underline{\underline{S}} - \underline{\underline{X}})}$  (3) with  $\underline{\underline{S}} = \underline{\underline{\sigma}} - \frac{1}{3} \text{tr} \underline{\underline{\sigma}} \underline{\underline{1}}$  (4)
- Flow rule :  $\dot{\underline{\underline{\epsilon}}}^p = \dot{p} \underline{\underline{n}}$  (5) with  $\underline{\underline{n}} = \frac{3}{2} \frac{\underline{\underline{S}} - \underline{\underline{X}}}{J_2(\underline{\underline{\sigma}} - \underline{\underline{X}})}$  (6) and  $\dot{p} = \sqrt{\frac{2}{3} \dot{\underline{\underline{\epsilon}}}^p : \dot{\underline{\underline{\epsilon}}}^p}$  (7)
- Isotropic hardening:  $\dot{R} = b (R_\infty - R) \dot{p}$  with  $R(0)=R_0$  (8)
- Kinematic hardening:  $\dot{\underline{\underline{X}}}_i = \frac{2}{3} C_i \varphi(p) \dot{\underline{\underline{\epsilon}}}^p - \gamma_i \underline{\underline{X}}_i \dot{p}$  (9)
- $\varphi(p) = 1 + (\psi - 1) e^{-bp}$  (10)

The model is used in an elastoplastic formulation with two kinematic variables.

-The NLK model modified by Burlet- Cailletaud [2] and used by Geyer [3] (named NLKBC model):

In this model, the kinematic hardening rule is changed and the other equations remain the same. It is a combination of the NLK model and a model due to Burlet-Cailletaud [2] which introduces a radial evanescence remain term in the non linear kinematic hardening rule:

$$\dot{\underline{\underline{X}}}_i = \frac{2}{3} C_i \varphi(p) \dot{\underline{\underline{\epsilon}}}^p - \gamma_i [\delta_i \underline{\underline{X}}_i + (1 - \delta_i) (\underline{\underline{X}}_i : \underline{\underline{n}}) \underline{\underline{n}}] \dot{p}$$

with  $\varphi(p) = 1 + (\psi - 1) e^{-bp}$  (11)

and  $\underline{\underline{n}}$  : normal to the yield surface  $\delta_i$  : a new parameter

The model is used in an elastoplastic formulation with two kinematic variables.

-The NLK model modified by Ohno-Wang [4] (named NLKOW model):

In this model, Ohno and Wang modify the kinematic hardening rule, considering that each component of back stress  $\underline{\underline{X}}_i$  has a critical state for its recovery to be fully activated.

Dynamic recovery is activated non linearly as its magnitude is lower than  $r_i$ .

$$\dot{\underline{\underline{X}}}_i = \frac{2}{3} C_i \dot{\underline{\underline{\epsilon}}}^p - \gamma_i \varphi(p) \left( \frac{\underline{\underline{X}}_i}{r_i} \right)^{m_i} < \dot{\underline{\underline{\epsilon}}}^p : \underline{\underline{k}}_i > \underline{\underline{X}}_i$$

with  $\varphi(p) = \varphi_\infty + (1 - \varphi_\infty) e^{-bp}$  (14)

$$\text{with } I_i = \frac{C_i}{\gamma_i \phi(p)} \quad (15) \quad \bar{X}_i = \sqrt{\frac{3}{2} \underline{X}_i : \underline{X}_i} \quad (16) \quad \underline{k}_i = \frac{\underline{X}_i}{\bar{X}_i} \quad (17)$$

$\langle \cdot \rangle$  are the Mac Cauley bracket:  $\langle u \rangle = u$  if  $u > 0$  and  $\langle u \rangle = 0$  if  $u < 0$

This model is used here in an elastoviscoplastic formulation including strain memory effects (the corresponding equations are not reported here; they are presented in [4]).

-The NLK model modified by Benallal -Marquis [5] and by Calloch [6], named NLKC:

This model, (as the following one) has only one non linear kinematic hardening rule :

$$\dot{\underline{X}} = C ( \underline{\epsilon}_p - \phi(p) \underline{X} ) \dot{p} \quad (18)$$

$$\text{with } \phi(p) = \phi_\infty + (\phi_0 - \phi_\infty) e^{-wp} \quad (19)$$

In this model, a nonproportionality parameter A is introduced to describe the nonproportionality of the loadings :

$$A = 1 - \frac{(\underline{X} : \dot{\underline{X}})^2}{(\underline{X} : \underline{X}) (\dot{\underline{X}} : \dot{\underline{X}})} \quad (20)$$

Then, the asymptotic value Q of the isotropic variable R, constant in the NLK model, is now considered as a new strain hardening variable which evolution law depends on the nonproportionality factor A. Thus, the isotropic hardening rule depends on the degree of nonproportionality of the loading and it becomes :

$$\dot{R} = \gamma (Q_\infty - R) \dot{p} \quad (21)$$

$$\dot{Q} = D(A) (Q_{AS}(A) - Q) \dot{p} \quad \text{with } D(A) = (d-f) A + f \quad (22)$$

$$Q_{AS}(A) = \frac{gAQ_\infty + (1-A) Q_0}{gA + (1-A)} + [ A^n (1-A) Q_i + A (1-A)^n Q_j ] \quad (24)$$

The other equations remain unchanged. The model is used in an elastoplastic formulation.

- The NLK model modified by Tanaka [7], named NLKT:

To describe the nonproportional hardening, he introduces an internal structural second rank tensor  $\underline{C}$ , and define a nonproportionality parameter A using this tensor and the normalized inelastic strain rate vector,  $\underline{u}$ .

$$A = \sqrt{\frac{\text{Tr}(\underline{C}^T \underline{C}) - \underline{u} : \underline{C}^T \underline{C} \underline{u}}{\text{Tr}(\underline{C}^T \underline{C})}} \quad (25)$$

$$\dot{\underline{C}} = c_c \left[ \left( \frac{\dot{\underline{E}}^p}{\|\dot{\underline{E}}^p\|} \otimes \frac{\dot{\underline{E}}^p}{\|\dot{\underline{E}}^p\|} \right) - \underline{C} \right] \dot{p} \quad (26) \quad \text{and } \underline{E}^p : \left\{ \begin{array}{l} E_1 = \epsilon_{11}^p \\ E_2 = \frac{2}{\sqrt{3}} [ \epsilon_{11}^p / 2 + \epsilon_{22}^p ] \\ E_3 = 2 \epsilon_{12}^p / \sqrt{3} \\ E_4 = 2 \epsilon_{23}^p / \sqrt{3} \\ E_5 = 2 \epsilon_{31}^p / \sqrt{3} \end{array} \right. \quad (27)$$

He also describes the amplitude dependence of the cyclic hardening and introduces two new internal variables,  $\underline{Y}$  and  $q$ , respectively the center and the range of a new index surface in the plastic strain space.

$$\left\{ \begin{array}{l} \dot{\underline{Y}} = r_y ( \underline{E}^p - \underline{Y} ) \dot{p} \\ q = \|\underline{E}^p - \underline{Y}\| \end{array} \right. \quad (28)$$

Then, the asymptotic value  $Q$  of the isotropic hardening variable  $R$  is governed by the variables  $A$  and  $R$  only and expresses as :

$$\begin{cases} \dot{R} = d_H (Q - R) \dot{p} & (29) \\ Q = A [q_N(q) - q_P(q)] + q_P(q) & (30) \end{cases}$$

where  $q_N(q)$  is the target value from the case of nonproportional hardening ( $A=1$ ) and on the other hand  $q_P(q)$  is the value for proportional hardening ( $A=0$ ).

$E = 168\,500 \text{ MPa}$	$R_0 = 163 \text{ MPa}$	$C_1 = 4822 \text{ MPa}$	$C_2 = 224 \text{ MPa}$
$\nu = 0.3$	$R_\infty = 163 \text{ MPa}$	$a_1 = 74$	$a_2 = 150$
$\delta_1^* = 2 \text{ E-}04$ $\delta_2^* = 1$	$b = 10$	$\omega = 6$	$\psi = 0.41$

Table 2: Material parameters of the NLK and the NLKBC model  
These models have the same parameters except  $\delta_1$  and  $\delta_2$  for the NLKBC model

$E = 192\,000 \text{ MPa}$	$Q_0 = -1.38 \text{ MPa}$	$C_1 = 69208.9 \text{ MPa}$	$m_1 = 21.1$
$\nu = 0.3$	$Q_{\max} = 372.1 \text{ MPa}$	$\gamma_1 = 697.7$	$m_2 = 8.51$
$k = 112.7 \text{ MPa}$	$\phi_\infty = 1$	$C_2 = 6603.4 \text{ MPa}$	
	$b = 13.2$	$\gamma_2 = 61.7$	

Table 3: Material parameters of the NLKOW model

$E = 187\,000 \text{ MPa}$	$Q_0 = 0 \text{ MPa}$	$d = 90$	$\omega = 10.0$
$\nu = 0.33$	$Q_\infty = 214 \text{ MPa}$	$d = 0.1$	$C = 61845 \text{ MPa}$
$k = 160 \text{ MPa}$	$Q_i = 2334 \text{ MPa}$	$\phi_\infty = 0.48\text{E-}02$	$(\phi_0 - \phi_\infty) = 0.65\text{E-}02$
$\gamma = 32$	$n = 8.26$	$f = 0.85$	

Table 4: Material parameters of the NLKC model

$E = 187\,000 \text{ MPa}$	$d_H = 32$	$a_P = 0$	$\phi_\infty = 0.48\text{E-}02$
$\nu = 0.33$	$a_N = 77300$	$b_P = 0$	$(\phi_0 - \phi_\infty) = 0.65\text{E-}02$
$k = 160 \text{ MPa}$	$b_N = 50.7$	$c_P$	$\omega = 10$
$c_C = 2.1$	$c_N = 6377.7$	$C = 61845 \text{ MPa}$	$r_\gamma = 40.75$

Table 5: Material parameters of the NLKT model

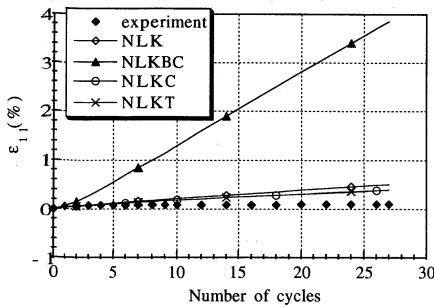


Fig. 8: Simulations with different models: Maximal axial strain over a cycle versus the number of cycles. path I - phase 1.

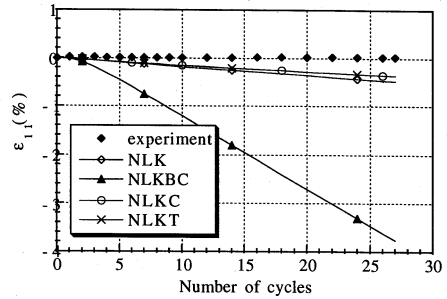


Fig. 9: Simulations with different models: Maximal axial strain over a cycle versus the number of cycles. path II - phase 1.

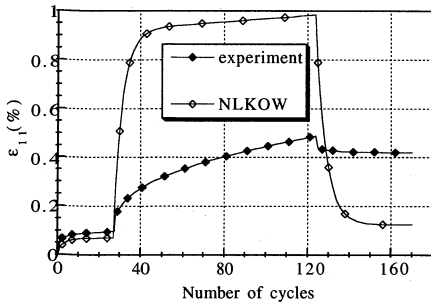


Fig. 10: Simulations with NLKOW model Maximal axial strain over a cycle versus the number of cycles. path I .

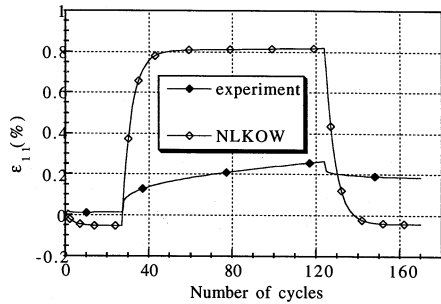


Fig. 11: Simulations with NLKOW model Maximal axial strain over a cycle versus the number of cycles. path II.

Axial	strain	experiment	NLK model	NLKBC model	NLKC model	NLKT model	NLKOW model
	end of phase 1	0.0740	0.4917	3.8613	0.3743	0.3744	0.0479
path I	end of phase 2	0.4676	24.756	20.290	14.279	16.821	0.9105
	end of phase 3	0.3996	25.455	26.801	14.746	17.217	0.1038
	end of phase 1	-0.0082	-0.4917	-3.8613	-0.3743	-0.3744	-0.0374
path II	end of phase 2	0.2400	4.2752	-16.771	11.372	14.192	0.8124
	end of phase 3	0.1620	3.4723	-23.970	10.811	13.625	-0.0374

Table 6 : Axial strain (%) at the end of each phase - Simulations and measurements

## MODELS IDENTIFICATION

The material parameters required by the different phenomenological models are presented in table 2 to 5. For the NLK, NLKBC, the NLKOW models, the parameters have been identified on another Stainless Steel close to our material; the identification is presented in [8]. For the NLKC and NLKT models, they have been identified by Calloch [7] on the material tested here.

## PREDICTION OF THE TESTS

We first evaluate the performance of these different constitutive equations in comparing the maximal axial strain over each cycle measured experimentally and obtained by the simulations. For both path I and II, the NLK, NLKBC, NLKC and NLKT models give poor predictions of the experimental results (see figures 8, 9 and table 6) : they overestimate the experimental rate of ratchetting, during the three phases; the NLKBC model even gives negative ratchetting during phase 2 of path II. Conversely, the NLKOW model reproduces fairly well phase 1 and 2 (see figures 10 and 11). But it fails to describe correctly phase 3 : it gives a complete recovery of the axial strain unlike the experimental results (see figure 10).

## CONCLUSIONS

Two nonproportional bowtie type tension-torsion tests are carried out on 316 Stainless Steel tubes combining simultaneous cycling of the axial stress and shear strain at three different mean stress and the same shear strain amplitude. We observe ratchetting of the axial strain during the two paths.

Five phenomenological models are tested. The NLK, NLKBC, NLKC and NLKT models fail to describe correctly the experimental results. The NLKOW gives good results for the tests but predicts a complete recovery of the axial strain in the last part of the tests unlike the experimental results.

## REFERENCES

1. Chaboche J.L., 1989. Constitutive equations for cyclic plasticity and cyclic viscoplasticity. *International Journal of Plasticity*, 5, 247-302.
2. Geyer P., 1995. On use of radial evanescence remain term in kinematic hardening. *Proc. 13th SMIRT: Vol. II*, 699-704. Porto Allegre, Brasil.
4. Ohno N., Wang J.D. 1993. Kinematic hardening rules with critical state of dynamic recovery, Parts I and II. *International Journal of Plasticity*, 9, 375-390.
5. Tanaka E., 1994. A Nonproportionality Parameter and a Viscoplastic Constitutive Model Taking into Account Amplitude Dependence and Memory Effects of Isotropic Hardening. *European Journal of Mechanics, and Solids*, 13, 155-173.
6. Benallal A., Marquis D. 1987, Constitutive Equations for Nonproportional Cyclic Elasto-Viscoplasticity. *ASME, Journal of Engineering Materials and Technology*, 109, 326.
7. Calloch S., Marquis D. 1996. Triaxial Tension-Compression Loading in Cyclic Elasto-Plasticity: Experimental and Numerical Aspects. *Proc. of the 3rd Asia-Pacific Symposium on Advances in Engineering Plasticity and its Applications*, 135-141.
8. Cabillat M.T., Geyer P., Robinet P., Migne C., Matheron P., Yuritzinn T. and Taheri S. Benchmark on thermal ratchetting test. Comparison of different constitutive models. *SMIRT 97 Paper LA03*, Lyon France.